Abnormal Compartmentalization of Cartilage Matrix Components in Mice Lacking Collagen X: Implications for Function

Kin Ming Kwan,* Michael K.M. Pang,‡ Sheila Zhou,§ Soot Keng Cowan,* Richard Y.C. Kong,* Tim Pfordte,‖ Bjorn R. Olsen,‖ David O. Sillence,¶ Patrick P.L. Tam,§ and Kathryn S.E. Cheah*

*Biochemistry Department and ‡Oral Biology Unit, The University of Hong Kong, Hong Hong; §Children's Medical Research Institute, Wentworthville, N.S.W. 2145, Australia, and ‖Department of Cell Biology, Harvard University, Boston, MA; and ¶Department of Clinical Genetics, New Children's Hospital, Westmead, NSW 2145, Australia

Abstract. There are conflicting views on whether collagen X is a purely structural molecule, or regulates bone mineralization during endochondral ossification. Mutations in the human collagen α1(X) gene (*COL10A1*) in Schmid metaphyseal chondrodysplasia (SMCD) suggest a supportive role. But mouse collagen α1(X) gene (*Col10a1*) null mutants were previously reported to show no obvious phenotypic change. We have generated collagen X deficient mice, which shows that deficiency does have phenotypic consequences which partly resemble SMCD, such as abnormal trabecular bone architecture. In particular, the mutant mice develop *coxa vara*, a phenotypic change common in human SMCD. Other consequences of the mutation are reduction in thickness of growth plate resting zone and articular cartilage, altered bone content, and atypical distribution of matrix components within growth plate cartilage. We propose that collagen X plays a role in the normal distribution of matrix vesicles and proteoglycans within the growth plate matrix. Collagen X deficiency impacts on the supporting properties of the growth plate and the mineralization process, resulting in abnormal trabecular bone. This hypothesis would accommodate the previously conflicting views of the function of collagen X and of the molecular pathogenesis of SMCD.

Endochondral ossification is the major process leading to the formation and growth of most of the skeleton in vertebrates during skeletogenesis. This process involves gradual replacement of the primordial cartilaginous model in the growth plate by bony tissue through temporally and spatially coordinated differentiation, growth, and remodeling events of chondrocyte proliferation, maturation, and hypertrophy. During the final stages of this process, calcification of hypertrophic cartilage occurs, vasculature invades, and bone matrix is deposited, replacing the cartilaginous matrix at the chondro-osseous junction of the growth plate (Iannotti, 1990).

Collagen X is a homotrimer of three α1(X) chains, with a short (38 aa) nonhelical amino terminus (NC2), a triple helix of 463 aa and a COOH-terminal highly conserved noncollagenous domain (NC1) of 161 aa. This collagen is the major extracellular component synthesized by hypertrophic chondrocytes in growth cartilage destined to be calcified and in zones of secondary ossification (Mayne and Irwin, 1986; Schmid and Linsenmayer, 1987). Expression of the α1(X) collagen gene is specifically associated with hypertrophic chondrocytes and precedes the onset of endochondral ossification (Kong et al., 1993). Although this collagen does not form fibrils, it has been found as fine pericellular filaments in association with cartilage collagen fibrils (Schmid and Linsenmayer, 1990). Collagen X molecules may also form other supramolecular structures in the matrix, since they have been shown to assemble into a hexagonal lattice in vitro (Kwan et al., 1991).

Apart from association with collagen fibrils, collagen X interacts with other matrix components, such as annexin V, chondrocalcin (Kirsch and Pfäffle, 1992) and proteoglycans (Chen et al., 1992). Collagen X has been shown to enhance accumulation of proteoglycans when it infiltrates into nonhypertrophic cartilage (Chen et al., 1992). Collagen X has also been shown to be intimately associated with the calcification process by binding to Ca^{++} and matrix vesicles, which are cell-derived microstructures found in the matrix of calcifying cartilage and bone and thought to be important in the initiation of mineral deposition (Anderson, 1989). In addition, the expression of collagen X precedes mineral deposition by cultured chondrocytes (Kirsch et al., 1992).

Despite the wealth of information about collagen X, the precise function of this protein and its role in the patho-

Please address all correspondence to K.S.E. Cheah, Biochemistry Department, The University of Hong Kong, Sassoon Road, Hong Kong. Tel.: 852 281991170/240. Fax: 852 285 51254. E-mail: hrmbdkc@hkuxa.hku.hk

The present address of R.Y.C. Kong is Department of Applied Biology, City University, Tat Chee Avenue, Hong Kong.

© The Rockefeller University Press, 0021-9525/97/01/459/13 $2.00

genesis of chondrodysplasia, has remained the subject of controversy. Because of its specific association with hypertrophic chondrocytes in the calcifying zone of growth plate cartilage, collagen X has been proposed to be important for endochondral bone formation (Schmid and Linsenmayer, 1987). Proposed functions include, providing an easily resorbed fabric for the deposition of bone matrix during endochondral growth of long bones; providing support as the cartilage matrix is degraded during endochondral ossification (Gibson et al., 1986; Schmid and Linsenmayer, 1985); or regulating the calcification process during endochondral ossification (Bonen and Schmid, 1991; Schmid et al., 1991; Poole and Pidoux, 1989; Schmid et al., 1990). Reconciling these different views has also been difficult because the consequence of gene mutations which result in collagen X deficiency in human and mouse are contradictory.

Mutations in the NC1 encoding domain of the human α1(X) collagen gene (*COL10A1*) have been found to be associated with the autosomal dominant inherited skeletal disorder, Schmid metaphyseal chondrodysplasia (SMCD)[1] (Warman et al., 1993; Wallis et al., 1994; Wallis, 1993; McIntosh et al., 1995). SMCD is a relatively mild form of metaphyseal chondrodyplasia, resulting from growth plate abnormalities. The SMCD phenotype is variable in severity and characterized by short to normal stature, with *genu varum* (bow legs), *coxa vara* (a reduced angle between the femoral neck and shaft), and flaring of the metaphyses of long bone (Lachman et al., 1988; Horton and Hecht, 1993). Transgenic mice expressing truncated chicken collagen X, display much more severe skeletal abnormalities, similar to human spondylometaphyseal dysplasia (SMD) (Jacenko et al., 1993*b*), in which there is reduced thickness of the hypertrophic zone of the growth plate and a decrease in newly formed bony trabeculae.

Since collagen α chains associate via the NC1 domain, it has been proposed that in human SMCD, the NC1 mutations result in failure of trimer assembly (Warman et al., 1993; Wallis et al., 1994) and the phenotypic changes are caused because collagen X is depleted in the matrix. This proposal is supported by recent reports that collagen α1(X) chains carrying SMCD mutations are unable to form trimers in in vitro assembly and cell transfection experiments (Chan et al., 1995, 1996). In the SMD transgenic mice, the chondrodysplasia is postulated to be caused by a depletion of collagen X as a result of instability/degradation of mutant chicken-mouse hybrid protein or because the chicken α chains interfere with the normal assembly of mouse collagen X.

Haploinsufficiency for collagen X as the cause of SMCD would be consistent with a supportive role for this protein (Warman et al., 1993; Wallis et al., 1994; Jacenko et al., 1993*a*). Therefore it was suprising to find that mice carrying a null mutation in the α1(X) collagen gene (*Col10a1*) have been reported to show no abnormality and no signs of SMCD (Rosati et al., 1994). This finding suggests that collagen X does not play a structural role by providing support in the growth plate.

To gain insight into the function of collagen X, we have created a null mutation in mouse *Col10a1* by homologous recombination in ES cells. To resolve the apparently contradictory consequences of mutations in the gene of human and mouse and gain better insight into the pathogenesis of SMCD, we have focused our study on the consequences of collagen X deficiency on the structure of the growth plate and trabecular bone, and on the organization of matrix components within cartilage.

In this study we have found that collagen X deficiency does have phenotypic consequences in mice. Some of the abnormalities partly resemble those found for human SMCD. Our data help address issues raised by the apparent discrepancy in phenotype between human and mouse and in addition, reveal insight into the function of collagen X. Based on the present findings, we propose that collagen X plays a role in the normal distribution of the cartilage matrix components within the growth plate. Deficiency of this collagen impacts on the supporting properties of the growth plate and the mass of newly formed trabecular bone, resulting in abnormal bone architecture.

Materials and Methods

Production of Collagen X Deficient Mice

A replacement gene targeting vector was generated from a cosmid clone containing the *Col10a1* gene (Kong et al., 1993) isolated from a 129Sv mouse genomic library (Fig. 1 *A*). It contained 7.6 kb of *Col10a1* sequence extending from 1.6 kb upstream of exon 1 to a HindIII site within exon 3; a neomycin resistance expression cassette (PGKneo, with the mouse *Pgk-1* gene promoter and polyadenylation site), inserted in reverse transcriptional orientation into EcoRI site of exon 3 (encodes the helical and COOH-terminal noncollagenous domains of the α1(X) collagen chain); and a herpes simplex virus thymidine kinase (tk) expression cassette (MC1tkpA) immediately 3′, to enrich for homologous recombinants by negative selection in FIAU. Targeted mutation of *Col10a1* would therefore result in a new BglII site and multiple stop codons in the coding region for the triple helix. The targeting vector DNA (25 μg) was linearized at a unique SalI site adjacent to the tk cassette and electroporated into 10^7 CCE ES cells (a gift of Dr. E. Robertson, Harvard University, Boston, MA) at 240V/500 μF using a gene pulser (Bio-Rad Labs., Hercules, CA). Recombinants were then double-selected by culturing in media containing 400 μg/ml G418 (GIBCO-BRL, Gaithersburg, MD) and 0.2 μM FIAU (Bristol-Myers Squibb, Wallingford, CT). Clones (480) were analyzed by HindIII digestion of genomic DNA and Southern hybridization to an internal 1.2-kb EcoRI-HindIII probe (Fig. 1 *A*) which hybridizes to a 4.9-kb or a 3.3-kb fragment in the mutant and wild-type alleles, respectively. Correct targeting was confirmed using a 3′ probe (634 bp HindIII fragment) external to the targeted region, which hybridizes to two BglII fragments, 2.8 kb and 3.2 kb, in mutant instead of 6.0 kb and 3.2 kb in wild-type alleles (Fig. 1, *A* and *B*). Targeted ES clones were microinjected into C57BL/6 blastocysts to generate chimeras to obtain germline transmission. Germline chimeras were subsequently bred with both C57BL/6 and 129/SvJ females to produce mouse lines of C57BL/6-129/SvJ hybrid and pure 129/SvJ background, respectively. F1 agouti offspring carrying the *Col10a1* mutation were identified by Southern analysis on tail DNA using both internal and external probes. Heterozygous *Col10a1*$^{+/-}$ F1 progeny were mated to produce F2 litters containing homozygous null mutants (Fig. 1 *B*).

Reverse-Transcription PCR Assays

Total cartilage RNA was isolated from 2-d mice by the lithium chloride/urea method (Lovell-Badge, 1987). Reverse-transcription (RT)-PCR assays on cartilage RNA from 2-d mice, carried out as described previously (Kong et al., 1993), were used to determine if any wild-type *Col10a1* mRNA was transcribed from the mutant allele using primers specific to the sequence 3′ and 5′ to the PGKneo insert (Fig. 1 *A*, primer C [5′-ATACCTTCTCGTCCTTGCTT-3′] and primer A [5′-ACACAAAGGAGATATTGGCC-3′]) to yield an expected product of 417 bp. The

1. *Abbreviations used in this paper*: RHT, ruthenium hexammine trichloride; SCMD, Schmid metaphyseal chondrodysplasia; SMD, spondylometaphyseal dysplasia.

presence of mutant transcript was detected using primers C and B (5′-AGGGGAGGAGTAGAAGGTGG-3′) located within the PGKneo insert (Fig. 1 *A*) to give an expected product of 535 bp. Control reactions without reverse transcriptase were done in parallel. The 1.2-kb EcoRI–HindIII fragment (Fig. 1 *A*, *crossed box*) was used as a probe in Southern analyses to confirm that the resulting DNA bands corresponded to the wild-type and mutant *Col10a1* cDNA, respectively. PCR products amplified from DNA of wild-type and targeted ES cell clones using the two pairs of primers were used as an additional marker to confirm the sizes of the resulting RT-PCR products.

Immunohistochemistry, Morphometry, and Statistical Analyses

For immunostaining, 6-μm cryostat sections of Tissue-Tek OCT-embedded hindlimbs from 2-d mice were fixed in ice-cold 5% glacial acetic acid/95% ethanol and digested with testicular hyaluronidase (0.2% in PBS, Sigma type IV-S) for 30 min at room temperature. Specimens were treated with rabbit polyclonal antibody (diluted 1:500 in PBS/3%BSA, pH 7.2) against bacterially expressed COOH-terminal noncollagenous peptide of mouse collagen X (Pfordte, T., and B.R. Olsen, unpublished data) and the fluorescein isothiocyanate-conjugated goat anti-rabbit Ig (Southern Biotechnology Associates, Inc., Birmingham, AL; diluted 1:80 in PBS/3%BSA with 5% normal mouse serum). For histology, hindlimbs of 2-d, 4-wk, and 8-wk-old mice were fixed in 4% paraformaldehyde in PBS (pH 7.2). Samples from 2-d mice were processed without demineralization, but 4-wk and 8-wk samples were decalcified in 15% formic acid/0.5 M sodium formate. Specimens were embedded in Histo-resin (Jung). Sections (4 μm) were cut and stained with toluidene blue.

Morphometric measurement of the thickness of different zones of the growth plate and the articular cartilage was performed on sections (4 μm) of the limb stained with toluidine blue. Only sections in comparable longitudinal planes along the proximal-distal axis of the femur were chosen for morphometry. Camera lucida drawings of the distal region of the bone were made. The thickness of the zones, the numbers of trabeculae in the chondro-osseous junction, and columns of chondrocytes in the proliferating zone was determined by analyzing images captured by an ultrasonic digitizer (Grafbar) using a Stereometry program (Yucomp). Since sample sizes (n = 5–12) were relatively small, nonparametric comparison between groups of data was performed using Kolmogorov-Smirnov (K-S) test which examines if the distribution of the data was the same between genotypes. This test is sensitive to difference in median, dispersion, skewness between data sets but is not subject to any bias in ranking order. A two-tailed probability of <0.05 is taken to indicate significant difference in morphometric values between genotypes.

In Situ Hybridization

The expression of genes for several matrix molecules in the hindlimb of 2-d mutant mice of both genetic backgrounds was studied by in situ hybridization as previously described (Cheah et al., 1991). In brief, the tissues to be analyzed were fixed in 4% paraformaldehyde in PBS for 16 h at 4°C and embedded in paraffin and sectioned at 6 μm. Slides with sections were dewaxed and hybridized to [^{35}S]UTP-labeled RNA probes. Probes used were for: (*a*) collagens and matrix molecules normally expressed in cartilage: collagens α1(II), α1(IX), α1(X), α2(XI) (Cheah et al., 1991, 1995; Kong et al., 1993) α1(VI), α2(VI) (gifts of M.L. Chu, Thomas Jefferson University, Philadelphia, PA), osteonectin (gift of M. Kurkkinen, Wayne State University, Detroit, Michigan), aggrecan, link protein (gifts of Y. Yamada, National Institutes of Health, Bethesda, MD); and (*b*) for matrix molecules not normally expressed in cartilage: collagens α(I), α1(VIII), α2(VIII), and fibrillin (a gift of F. Ramirez, Mount Sinai School of Medicine, New York, NY). Hybridization, washing and RNase treatment followed as described (Cheah et al., 1991). Slides were dipped in emulsion (Ilford) and exposed for 2–20 d before developing.

Electron Microscopy

A total of eight mice, four mutant (−/−), and four wild-type (+/+) were studied. After sacrifice, tissues were immediately fixed in 5% glutaraldehyde, 2% paraformaldehyde with 0.05% ruthenium hexammine trichloride (RHT) in 0.1 M sodium cacodylate buffer (pH 7.3) for 6 h at 4°C and then rinsed in cacodylate buffer. After postfixation in 1% osmium tetroxide for 1 h, tissues were washed with buffer, dehydrated in ethanol, and then cleared in propylene oxide and embedded in resin. Ultrathin sections were produced using Reichert Ultracut S ultramicrotome and stained with uranium acetate and lead citrate. Sections were examined on a JEOL JEM-100 electron microscope operated at 80 kV. In addition samples from 3 −/− and 3 +/+ mice were fixed in tannic acid containing fixative as described (Rosati et al., 1994), instead of RHT and processed for electron microscopy.

Quantitation of Proteoglycans and Matrix Vesicles

The density of proteoglycan material (at a magnification of 50,000) in the upper hypertrophic zones of three wild-type and three mutant mice were measured by scoring the number of those proteoglycan granules and complexes touching a grid of 200 nm × 200 nm in a total tissue area of 3.2 μm^2

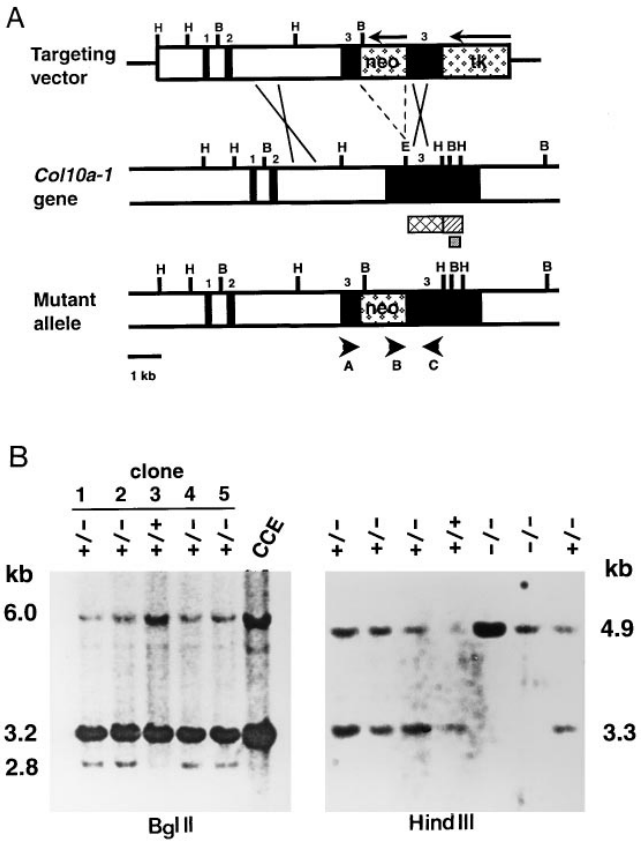

Figure 1. Targeted disruption of the *Col10a1* gene. (*A*) Targeting strategy and recombinant mutant allele of *Col10a-1*. Neomycin resistance (neo) and HSV-thymidine kinase (tk) genes (*spotted boxes*) with arrows indicating the direction of transcription. Restriction sites: *B*, BglII; *E*, EcoRI; *H*, HindIII. *Solid boxes*, exons of the gene; numerals above those boxes are exon numbers; *crossed box*, internal probe; *hatched box*, 3′ external probe; *gray box*, probe for in-situ hybridization; *arrowheads A*, *B*, and *C* show positions of primers used for RT-PCR analyses which revealed low levels of mutant transcripts in heterozygotes and homozygotes but no wild-type mRNAs in −/− mice. (*B*) *Left*, Southern analysis of representative ES cell clones by using 3′ external probe showing the 2.8 kb BglII fragment diagnostic of the mutant allele in targeted ES cell clones (clones 1, 2, 4, 5 ; +/−) and 6.0 kb BglII fragment being characteristic of wild-type allele (clone 3; +/+ and CCE) while the 3.2 kb BglII fragment is common for both wild-type and mutant alleles. *Right*, Southern analysis of tail biopsies of F2 mice from heterozygous cross by using internal probe showing the 4.9-kb HindIII fragment which is diagnostic of the mutant allele present in heterozygous (+/−) and homozygous (−/−) mutants but absent in wild-type (+/+) mice.

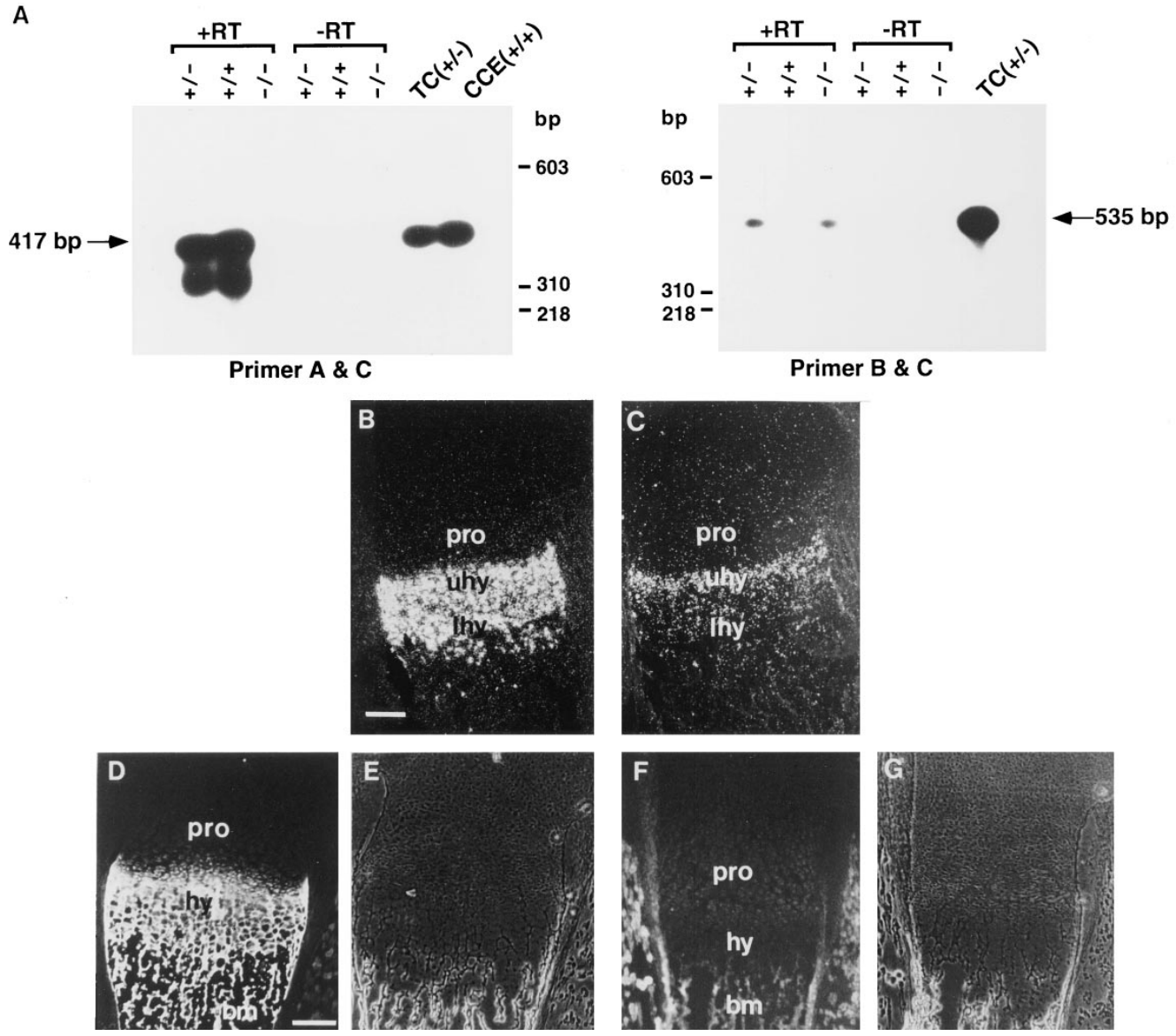

Figure 2. *Col10a1* mutant mice lacking collagen X. (*A*) RT-PCR analyses revealed no wild-type *Col10a1* mRNA transcript in the mutant mice (−/−) by using primers A & C (*left panel*); mutant *Col10a1* transcript was detected from heterozygous (+/−) and homozygous (−/−) by using primers B & C (*right panel*) but not from wildtype (+/+). *+RT*, with reverse transcriptase; *−RT*, without reverse transcriptase. *TC*, targeted ES cell clone DNA; *CCE*, wild-type ES cells DNA for PCR only as control for size. (*B* and *C*) Dark-field views of in situ hybridization on 2-d wild-type (*B*) and mutant (*C*) mice proximal tibia growth plate using α1(X) probe (see Fig. 1). A very low level of mutant *Col10a1* transcript was detected in mutant. Abbreviations: *pro*, proliferating chondrocytes; *uhy*, upper hypertrophic chondrocytes; *lhy*, lower hypertrophic chondrocytes. Bar, 200 μm. (*D* and *F*) Immunostaining of the growth plate cartilage of the proximal tibia of wild-type (*D*) and null mutant (*F*) show no detectable collagen X in the mutants but presence of the protein in the hypertrophic zone and cartilaginous remnants in bony trabeculae of wild type. (*E* and *G*) Phase contrast pictures of a region shown in *D* and *F*, respectively. Abbreviations: *pro*, proliferating zone; *hy*, hypertrophic zone; *bm*, bone matrix. Bar, 200 μm.

in five different fields. The number of matrix vesicles in a tissue unit volume of 0.32 μm^3 (magnification of 50, 000) were counted in seven mutant and seven wild-type mice (see Table II). The data were assessed for statistical significance by the two-tailed Mann-Whitney U test.

Radiological and Mineral Density Analyses

Contact X-ray microradiographs of 2-d and 4-wk intact limbs, fixed in 4% paraformaldehyde in PBS (pH 7.2), were taken using the Softex X-ray machine (Softex ISO-20, Japan) with ultra-high resolution photographic film (Kodak Spectro-photographic film). This method yields high resolution X-ray images but could not be used on larger bones from mice older than 4-wk. The exposure for 2-d samples was 5 min at 18 kV/3 mA and for 4-wk samples was 10 min at 18 kV/5 mA. X-ray images were captured digitally into a microcomputer using a light microscope equipped with a 3-CCD video camera (JVC-3800, Japan). Mineral density was computed using Image 1.7 software (Macintosh) and statistical analyses of the data computed by K-S test as for the morphometric measurements. A two-tailed probability of <0.05 is taken to indicate a significant difference in density values between genotypes.

Radiological images of older animals were taken under identical exposure and radiation energy (24 kV/25 mA) using high resolution Kodak mammography X-ray film (Kodak Diagnostic film Min-R^{TM}H MRH-1) and a General Electric X-ray machine (Senograph 600T Senix HF, General Electric). Mice

were briefly narcotized to facilitate radiography. To guard against artefact due to variation in positioning of the femur while taking X rays, a consistent position of the legs were maintained as far as possible and only comparable images in which the trochanter could be seen, were measured.

Results

Generation of Collagen X Deficient Mice

The mouse α1(X) collagen gene (*Col10a1)* spans 7.0 kb of DNA and contains three exons. Exons 2 and 3 together encode the entire translated sequence, with the triple helical and NC1 domains encoded within exon 3. To generate a null allele of *Col10a1*, a targeting vector was constructed that would generate a mutant allele with an exon 3, disrupted in the beginning of the helix encoding domain, and also containing multiple premature stop codons (Fig. 1 *A*). Eight targeted clones were identified by Southern blot hybridization using both internal and 3′ external probes (Fig. 1 *B*), at a frequency of 2% in G418 and FIAU-double resistance clones. Four targeted clones were used for generation of chimeric mice and two of them contributed to the germline (Fig. 1 *B*). Chimeras from two of these independently derived ES clones were subsequently bred with both C57BL/6 and 129/SvJ females to produce mouse lines of C57BL/6-129/SvJ hybrid and pure 129/SvJ background, respectively, in order to assess any difference in the phenotype of different genetic backgrounds. Heterozygous F1 *Col10a1*$^{+/-}$ appeared normal and were bred to produce homozygous F2 *Col10a1*$^{-/-}$ (hereafter termed mutant) which appeared superficially similar to wild type. Approximately 25% of F2 offspring were homozygous null mutants which could survive up to 2 years of age.

To assess if the mutant mice were truly deficient in collagen X, RT-PCR assays were used to determine if wild-type *Col10a1* mRNA was present using primers specific to sequences 3′ and 5′ to the PGKneo insert. No wild-type *Col10a1* transcript was detected in cartilage RNA (Fig. 2 *A*) in the mutant, although low levels of mutant *Col10a1* mRNAs were present (Fig. 2, *B* and *C*). The NC1 domain of collagen X has been shown to be important for trimer assembly (Chan et al., 1995). Cell transfection studies have shown that unassembled collagen X chains cannot be secreted and are degraded intracellularly (Chan et al., 1996). Therefore, any protein produced from mutant transcript would consist of the 38-aa NC2 domain only and probably would not be secreted to the matrix. Immunohistochemistry performed on the growth cartilage of 2-d-old mutant neonates showed absence of collagen X protein (Fig. 2, *D–G*) confirming the mice were deficient in the protein.

We tested for altered transcriptional activity for genes encoding eight other collagens and other matrix components which may have compensated for collagen X deficiency. These included genes for collagen α1(VIII) and α2(VIII) which are not normally expressed in cartilage but are structurally similar to collagen X (Muragaki et al., 1991*a*, *b*) and components not normally present in cartilage such as collagen α1(I) and fibrillin. In addition, enhanced expression of other genes expressed in cartilage such as collagens α1(II), α1(VI), α2(VI), α1(IX), α2(XI),

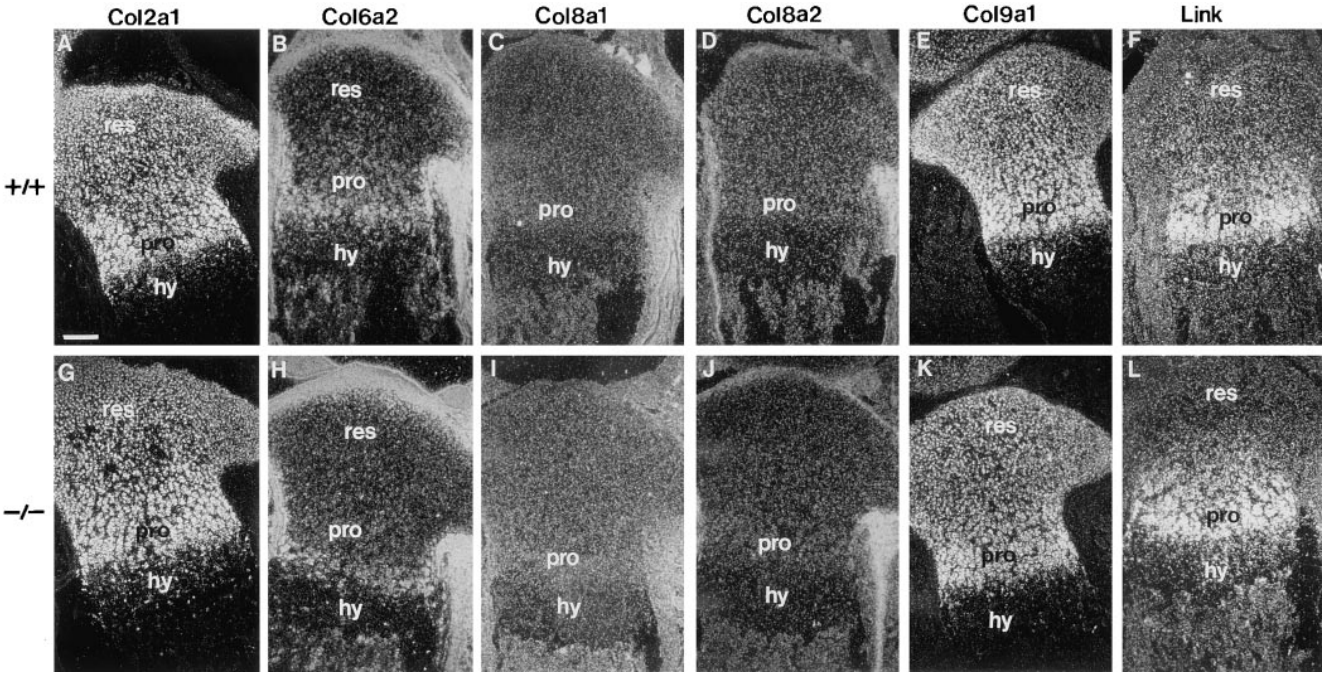

Figure 3. Unaltered transcriptional activity of other genes in the growth plate of collagen X mutants. In situ hybridization of proximal tibia growth plates of 129/SvJ 2-d-old wild-type (+/+, *A–F*) and mutant (−/−, *G–L*) mice showing expression of collagens α1(II) (*A* and *G*); α2(VI) (*B* and *H*); α1(VIII) (*C* and *I*); α2(VIII) (*D* and *J*); α1(IX) (*E* and *K*); and link protein (*F* and *L*). All pictures are dark-field views showing sections hybridized with corresponding matrix molecules antisense RNA probes. There is no alteration in the expression of these genes in the mutant mice compared with the wild type. Abbreviations: *res*, resting chondrocytes; *pro*, proliferating chondrocytes; *hy*, hypertrophic chondrocytes. Bar, 200 μm.

Table I. Growth Plate Measurements in Collagen X Deficient and Wild-Type Mice

	C011Oa-1 genotype			
	129Sv (*n*)		C57/BL6-129/SvJ (*n*)	
Zone 2 d pp	+/+ (8)	−/− (6)	+/+ (10)	−/− (12)
Resting	80.1 ± 1.5	65.8 ± 3.7*	71.1 ± 4.2	52.8 ± 4.3*
Proliferating + maturing	964.2 ± 23.3	999.2 ± 37.29	871.5 ± 46.6	800.7 ± 47.3
Hypertrophic	167.7 ± 5.3	187.5 ± 16.97	176.2 ± 12.4	173.0 ± 7.9
Total plate thickness	1211.0 ± 25.13	1252.5 ± 26.9	1118.8 ± 39.8	1026.5 ± 44.9
Width of plate	693.4 ± 39.5	749.2 ± 49.5	659.9 ± 43.5	666.5 ± 29.0
Number of columns	18.8 ± 1.3	19.6 ± 1.2	18.2 ± 1.2	17.7 ± 0.7
Number of trabeculae	19.6 ± 1.2	17.3 ± 0.7	16.4 ± 1.2	14.3 ± 0.9
4 wk	+/+ (10)	−/− (9)	+/+ (6)	−/− (11)
Articular cartilage	95.5 ± 11.9	77.5 ± 5.3	61.7 ± 4.3	51.5 ± 2.7*
Maturing	205.8 ± 11.0	184.2 ± 13.8	148.9 ± 6.1	147.9 ± 4.2
Hypertrophic	119.9 ± 8.7	108.5 ± 7.9	112.8 ± 8.4	110.0 ± 6.8
Total plate thickness	325.8 ± 14.1	292.7 ± 20.1	323.3 ± 14.8	309.4 ± 10.4
Number of trabeculae	18.30 ± 2.96	16.43 ± 0.90	19.33 ± 1.58	19.36 ± 0.65

A two-tailed probability of < 0.05 (denoted by *) by K-S test, is taken to indicate a significant difference in morphometric values between genotype. Values are mean ± SEM; units, μm; n = number of mice analyzed; +/+, wild type; −/−, homozygous null mutant.

osteonectin, aggrecan, and link protein was tested. In situ hybridization assays showed no changes in the distribution or levels of expression of those mRNAs in the growth plates of heterozygous or homozygous null mutant mice (Fig. 3 and data not shown).

Alterations in the Growth Plate and Trabecular Bone of Col10a1 Deficient Mice

The cellular development and overall architecture of growth plate cartilage of the femurs of 2-d and 4-wk-old mutant mice of two genetic backgrounds (C57BL/6-129/SvJ hybrid and 129/SvJ) appeared unchanged. However, detailed morphometric analyses revealed a 18–25% reduction in the height of the resting zone of chondrocytes in the epiphyseal growth plates in 2-d mutants of both genetic backgrounds (Table I). C57BL/6-129/SvJ hybrid 4-wk mutants showed a 17% reduction ($P < 0.05$ by K-S test) in articular cartilage thickness but there was less difference between mutant and wild-type in 4-wk 129/SvJ mice (Table I).

Histological analyses were made in four mutants and four wild-type mice at 2 d, 4 wk, and 8 wk. These analyses of the metaphyseal growth plate of the tibia of mutant mice have revealed alteration in the architecture of the trabecular bone at the chondro-osseous junction. In the 2-d 129Sv/J mutant, a more compact trabecular zone was found. There was also a reduced amount of bony material in the trabeculae and the bone marrow space was also reduced. There was, however, no obvious change in the cellularity of the marrow, except for a higher packing density of the marrow cells (Fig. 4, *A* and *B*). A compact trabecular region was still evident in 4-wk mutants (Fig. 4, *C* and *D*) and the amount of toluidine blue stained material in the trabeculae was similar between the mutant and wild-type tibia. By 8 wk, the trabeculae of wild-type mice had formed extensive ramifications and contained a much higher content of toluidine blue materials when compared with the mutant (Fig. 4, *E* and *F*). These morphological differences between wild-type and mutant mice were consistently found in the mice (four of each genotype) studied. However, such differences were less obvious in C57BL/6-129/SvJ hybrid mutant mice (data not shown).

Ultrastructural Abnormalities

To preserve the hydrated state of chondrocytes and stabilize macromolecular interactions between the plasma membrane and pericellular proteoglycans, thereby allowing better retention of matrix macromolecules, samples were fixed for electron microscopy in ruthenium hexammine trichloride (RHT) (Hunziker et al., 1982). Ultrastructural analyses revealed major changes in the distribution and organization of growth plate matrix materials. In 2-d-old null mutants of 129/SvJ background, there was a striking increased amount of matrix vesicles in the resting and proliferating zones of growth plate cartilage (Fig. 5, *A a–f*; Table II). Such matrix vesicles were absent in these zones of the wild-type mice and were normally found in the upper hypertrophic and maturing zones. In the mutant, there was a significant reduction in the quantity of the matrix vesicles in the upper hypertrophic zone of the growth plate cartilage (Fig. 5, *A g* and *h*; Table II). A similar pattern of abnormal distribution of proteoglycan-like material was also found. In the resting and proliferating zones of the mutant cartilage, the concentration of proteoglycan-like materials was markedly increased (Fig. 5 *A d* and *f*) but was reduced in the upper hypertrophic zone (Fig. 5 *A i* and *j*). Scoring measurements of the amount of proteoglycan granular material in the upper hypertrophic zone showed that there was a significant reduction in mutants compared with wild-type (two-tailed P value <0.05 by Mann-Whitney U test: mutant, 50.4 ± 2.2; wild type, 122.8 ± 22.0). Although the structure of collagen fibrils in the resting zone of wild-type and mutants were comparable (Fig. 5 *A a–d*), fibrils were organized differently in the proliferative and upper hypertrophic zones (Fig. 5 *A e–h*) which may be a consequence of the changed interactions between proteoglycans and other matrix components with the collagen fibrils. These differences were less pronounced in the

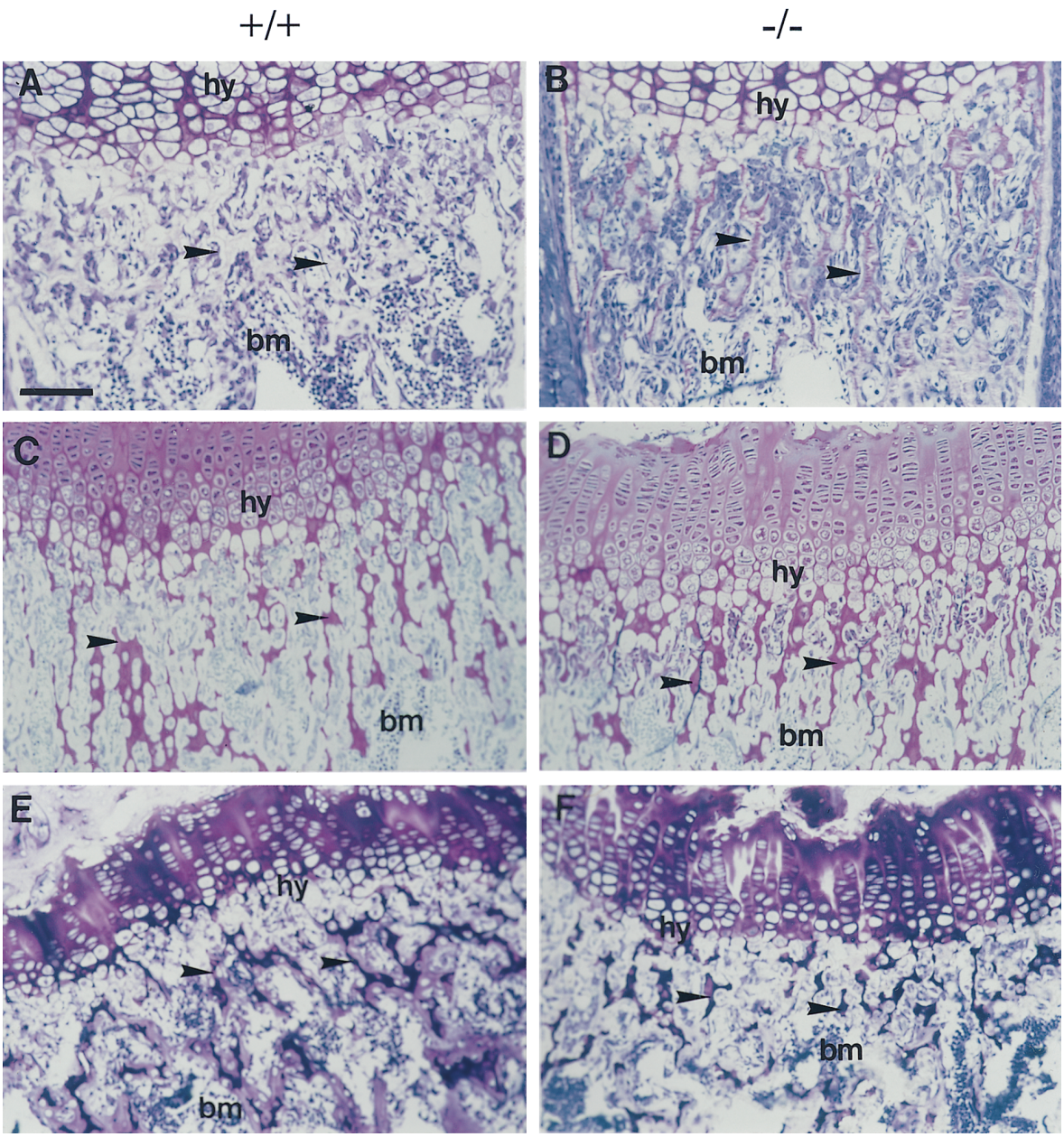

Figure 4. Altered trabecular morphology and organization in collagen X mutants. The proximal metaphyseal growth plate of the tibia was sectioned longitudinally and the matrix materials were stained with toluidine blue. (*A* and *B*) 2-d; (*C* and *D*) 4-wk and (*E* and *F*) 8-wk wild-type (+/+, *A*, *C*, and *E*) and mutant (−/−, *B*, *D*, and *F*) female mice of 129/SvJ background are shown. In mutants, the trabecular structure (*arrowheads*) appeared abnormal. Abbreviations: *hy*, hypertrophic chondrocytes; *bm*, bone marrow. Bar, 100 μm.

lower hypertrophic zone (Fig. 5 *A k* and *l*). In mutants, the mineral distribution in trabeculae was irregular and patchy (Fig. 5 *A m* and *n*), indicative of an altered deposition pattern. Nevertheless, the chondrocyte morphology and structure of different zones appeared normal in the mutants compared with the wild-type mice (data not shown). They did not display signs of a shift in differentiation program or of precocious necrosis or hypertrophy.

To visualize the fibrils better, proteoglycans and other matrix materials were preferentially removed by fixing samples in tannic acid. The elevated amount of granular materials seen in the proliferating zone of RHT-fixed mutant samples was not seen. However, a similar disorganization of collagen fibrils in the proliferating zone and atypical distribution of matrix vesicles were still evident in mutants (three −/− and three +/+ mice studied) (Fig. 5 *B d* and *f*). In addition the collagen fibrils appeared wavy and short. Although these phenotypic consequences in the mutant were not reported by Rosati et al. (1994), this may be related to differences in the genetic background of the mutant mice and the methodology of electron microscopic examination. In their studies, the morphology of the proliferating and resting zones of mutants were not examined. Futhermore, their samples were fixed in tannic acid, and therefore the abnormal distribution of proteoglycans would not be apparent.

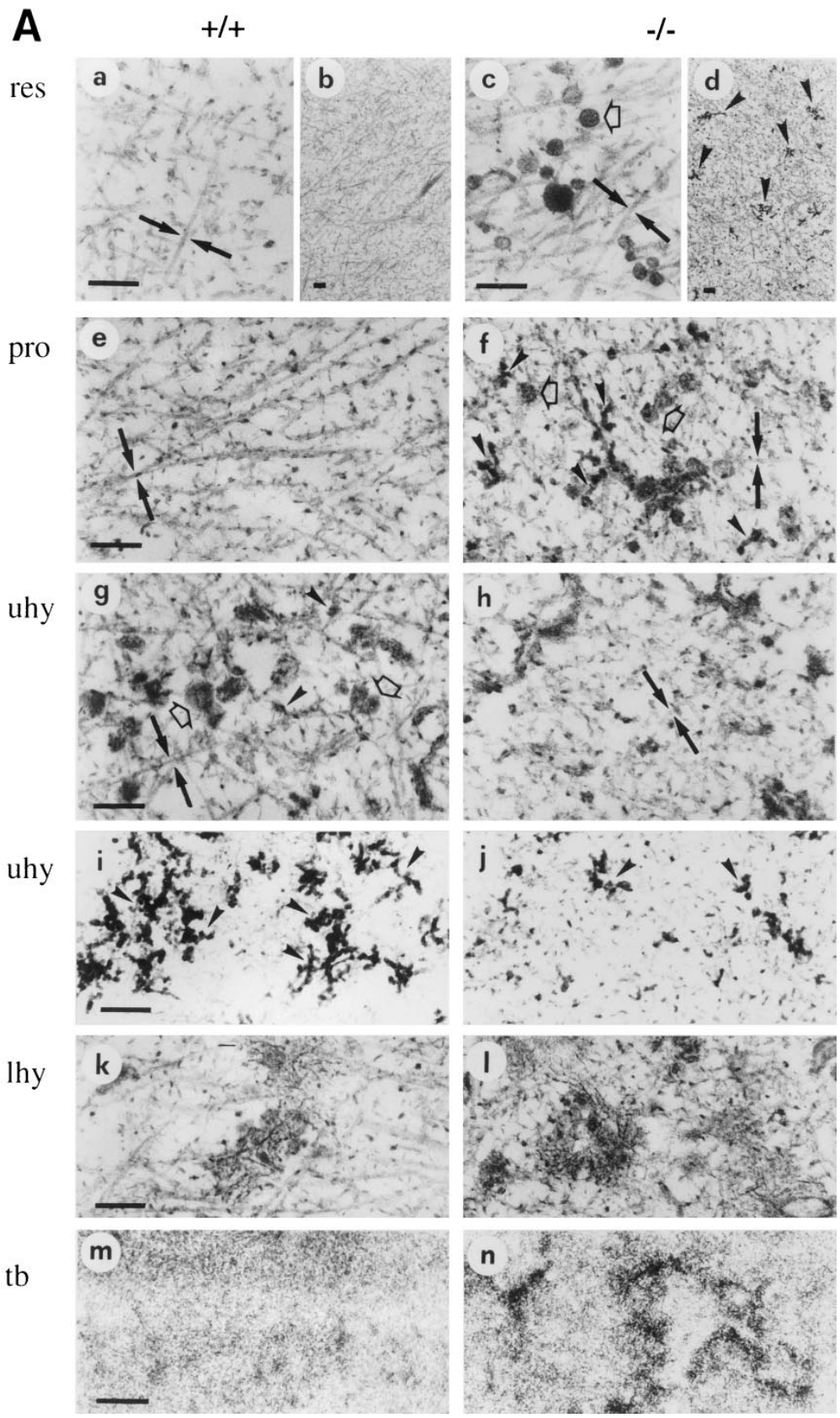
A
+/+
-/-
res
pro
uhy
uhy
lhy
tb
a
b
c
d
e
f
g
h
i
j
k
l
m
n

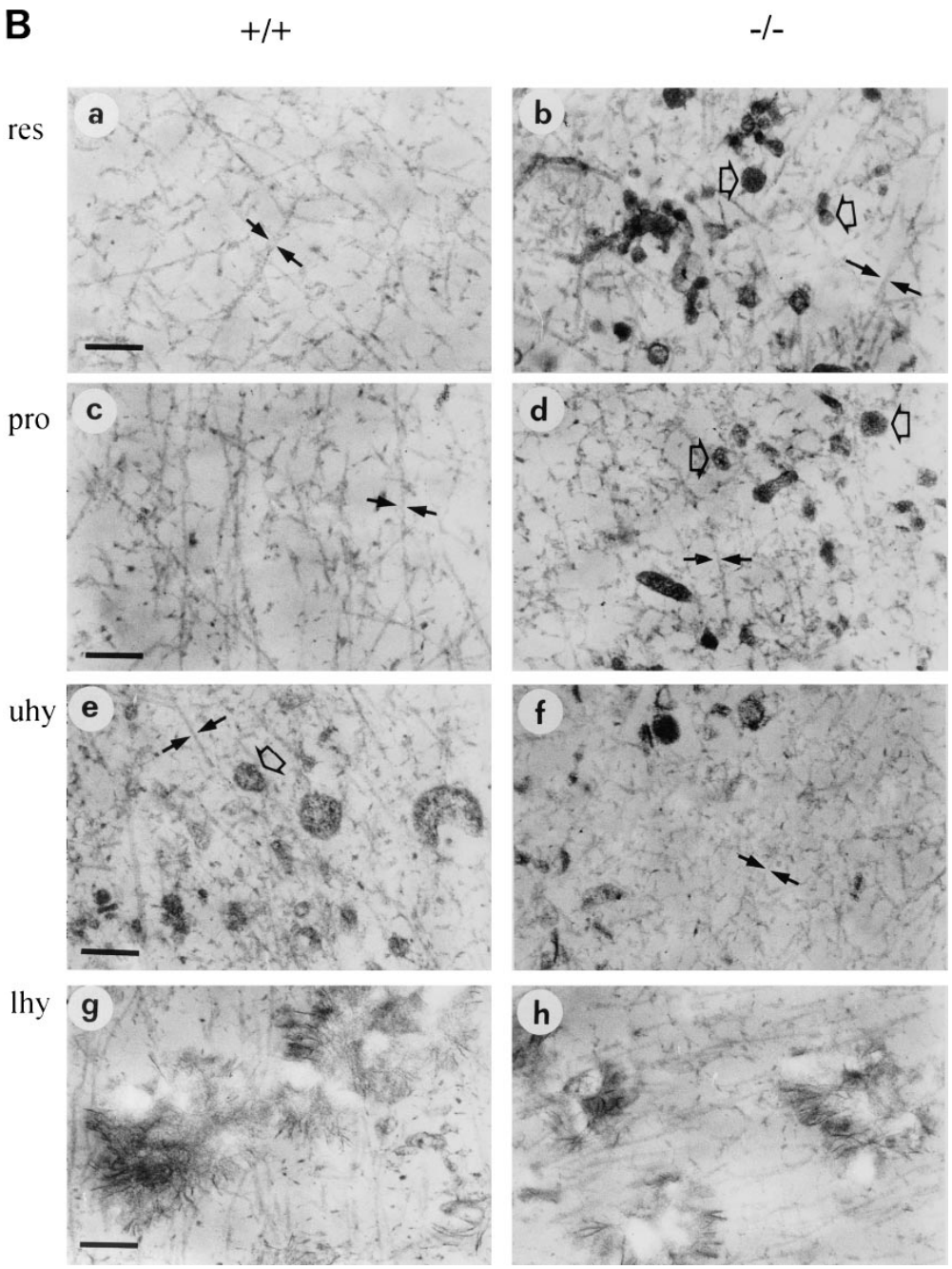

Figure 5. Altered distribution of proteoglycans and matrix vesicles in the growth plates of collagen X mutants. (*A*) Ultrastructure of the cartilage matrix of RHT-fixed samples from wild-type (+/+) and collagen X deficient (−/−) mice. Matrix ultrastructure of resting (*res*, *a–d*), proliferating (*pro*, *e* and *f*), upper hypertrophic (*uhy*, *g–j*), lower hypertrophic (*lhy*, *k* and *l*) zones of the growth plate cartilage and trabeculae (*tb*, *m* and *n*) of wild-type (+/+) and collagen X deficient (−/−) 2-d-old 129/SvJ mice are shown. In the four mutants studied, vesicles (*outlined arrowheads*), of average 100-nm-diam and containing electron-dense inclusions, characteristic of matrix vesicles, are more abundant in the matrix of the resting and proliferating zones, but are fewer in the upper hypertrophic zone (see Table II). Granular material (*filled arrowheads*), with the typical appearance of proteoglycans, some of which adhering to the surface of the collagen fibrils (*arrows*), are found dispersed in the matrix in all zones in the wild-type. The amount of these granular materials are increased in the mutant resting and proliferative zones (*d* and *f*) but reduced in the upper hypertrophic zone (*j*). Collagen fibrils in the proliferating and upper hypertrophic zones of the mutant are abnormal but are normal in the resting zone. Signs of mineralization in the form of calcified spicules can be seen in the lower hypertrophic zone (*k* and *l*) and in the trabeculae at the chondrosseous junction (*m* and *n*). Distribution pattern of mineral deposits in trabeculae of mutant is patchy compared to wild type. Bar, 200 nm. (*B*). Ultrastructure of the cartilage matrix of tannic acid–fixed samples from wild-type (+/+) and collagen X deficient (−/−) 2-d 129/SvJ mice. The specimens were fixed in a fixative, containing tannic acid, which in contrast to RHT fixative, would leach out proteoglycans. In the cartilage of the mutant mice, the membrane vesicles (*outlined arrowheads*) are found in the resting (*res*) and proliferating (*pro*) zones (*b* and *d*), in addition to the upper hypertrophic zone (*uhy*) where the membrane vesicles are normally compartmentalized (*a*, *c*, and *e*). The population of membrane vesicles in the upper hypertrophic zone of the mutant cartilage is also significantly reduced (*f*). Removal of the proteoglycan content in the cartilage revealed more clearly the fibrillar organization. In the resting zone, the fibrils (*arrows*) in the mutant and wild-type specimens display similar morphology (*a* and *b*), but the fibrils in the proliferating and upper hypertrophic zones of the mutant are more contorted and shorter in appearance (*d* and *f*). The ultrastructural appearance of the matrix in the lower hypertrophic zone is similar between the wild type (*g*) and the mutant cartilage (*h*). Bar, 200 nm.

Altered Bone Content and Coxa Vara in Col10a1 Deficient Mice

In view of the importance of matrix vesicles in the mineralization process, we investigated whether the ultrastructural and bone trabecular changes were accompanied by changes in bone content. The femurs of 2-d mutant and wild-type mice were examined by contact microradiography. These analyses revealed marked differences in the

Table II. Distribution of Matrix Vesicles in Different Tissue Compartments of the Growth Plate Cartilage of Limb Bones of Collagen X Deficient and Wild-Type Mice

Growth plate zone	Number of matrix vesicles/unit volume	
	+/+ (*n*)	−/− (*n*)
Resting	0 (14)	20.5 ±3.5* (11)
Proliferating	0 (12)	22.9 ± 4.1* (8)
Upper hypertrophic	18.9 ± 1.8 (12)	11.5 ± 1.7* (11)

*Significant difference (values at $P < 0.05$ by two-tailed Mann-Whitney U test) between +/+, wild-type; −/−, homozygous null mutant of 129/SvJ background; *n* = number of tissue fields studied; values are mean ± SEM; unit volume = area of tissue scored (3.2 μm^2) X section thickness (0.1 μm) = 0.32 μm^3.

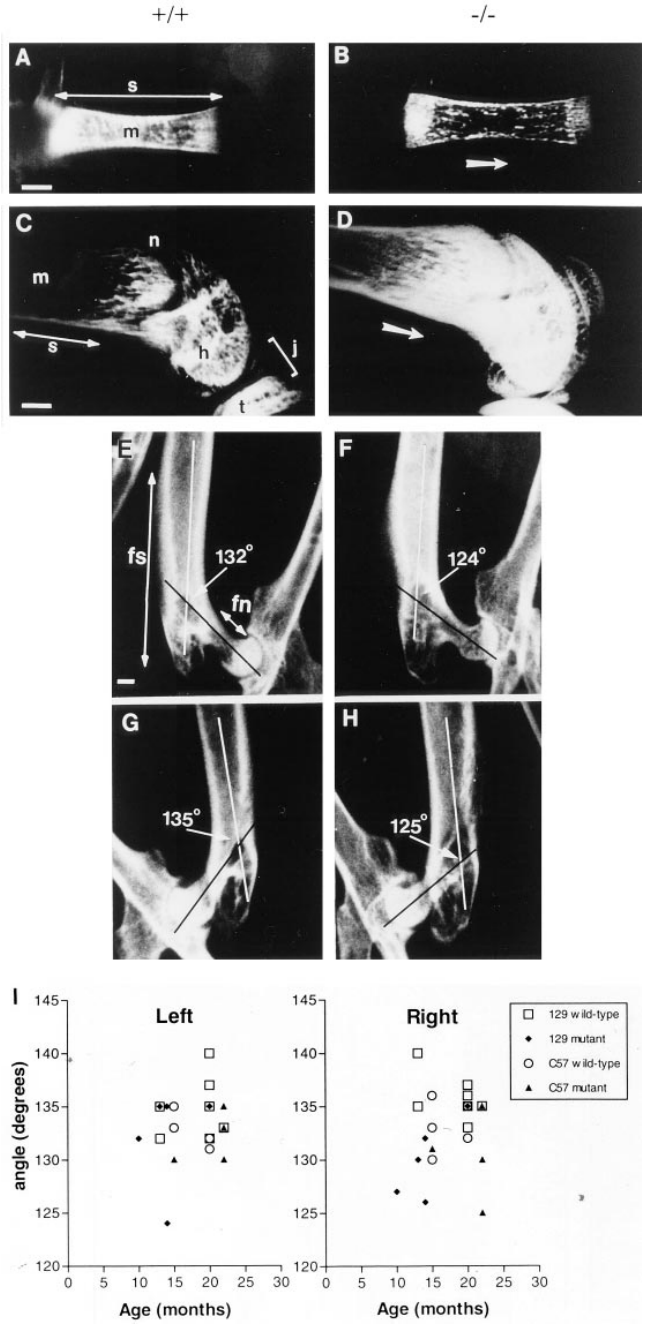

radiographic opacity of the trabecular bones of mutants. There was reduced overall bone content in the femur of 2-d 129/SvJ mutants (Fig. 6, *A* and *B*; Table III). But in 4-wk mutant femur, trabecular bone content was greater (Fig. 6, *C* and *D*; Table III). In C57BL/6-129/SvJ hybrid mutants bone content was decreased at 2 d but not at 4 wk (Table III).

A common feature of SMCD patients is the development of *coxa vara* which is clinically diagnosed as a reduction in the angle between the femoral neck and shaft, and a concordent shortening of the femoral neck. The hip joints of 13 wild-type and 10 collagen X deficient mice of both C57/BL6-129Sv/J hybrid and 129/SvJ background were examined radiographically (Fig. 6 *I*). When the angle of the femur was compared between the mutant and wild-type mice, without taking any consideration of the handedness of the bone, only a slight reduction in the angle was observed in the mutants. However, in three mutant mice, the angle measurement clearly fell outside the normal range expected from the wild type (Fig. 6, *F* and *H*). Moreover, when the left and right femurs were analyzed separately, statistically, there was a significant reduction in the angle for the right femur of the mutant mice (Mann-Whitney U test, $P < 0.05$; Fig. 6 *I*). Our study thus revealed a previously unnoticed unilateral *coxa vara* in some mice that lack collagen X.

Discussion

Skeletogenesis by endochondral ossification is a complex process involving coordinated events of signaling through various appropriate growth factors leading to the correct cellular development in the growth plate; synthesis of the appropriate matrix components; formation of a scaffold for initial and progressive deposition of mineral within the matrix; production of catabolic factors for removal and remodeling of the matrix—all in a precisely timed and spatially organized manner. Although details of the process of endochondral ossification are well described, our understanding of the molecular factors and mechanisms which

Figure 6. Altered bone content and incidence of *coxa vara* in collagen X mutants. (*A–D*) Microradiographs of the femurs of 2-d (*A* and *B*) and 4-wk (*C* and *D*) wild-type (+/+, *A* and *C*) and mutant (−/−, *B* and *D*) female mice of 129/SvJ background. The opacity of the bony region (white in X-ray image) correlates with the amount of radiographically opaque bone materials. The bone content was measured by densitometry at the sites indicated on the wild-type radiographs and the data are summarized in the Table III. Single-headed arrows in *B* and *D* indicate orientation proximal-distal. Abbreviations for bony landmarks: *h*, distal head (articular condyle); *j*, knee joint, *m*, marrow cavity; *n*, neck; *t*, tibia; *s*, shaft. Bar, 0.5 mm. (*E–H*) Radiographic study of the angle of the femur head of wild-type (+/+, *E* and *G*) and mutant (−/−, *F* and *H*) mice at 13–14 months (*E* and *F*) and 20–22 months (*G* and *H*). A decrease in the angle between the neck (*fn*) and the shaft (*fs*) of the femur (*coxa vara*) is observed at both ages. There is always a significant foreshortening of the length of the neck of the femur of the mutant mice shown in *F* and *H*. Bar, 1 mm. (*I*) Measurements of the angle of the head of the left and right femur of the wild-type and mutant mice at various postnatal ages. Significant unilateral (*right*) *coxa vara*, showing varus angulation was found in some collagen X deficient mutants (see Results).

Table III. Measurements of Radiographic Opacity in Collagen X Deficient and Wild-Type Mice

Bone and age (pp)	*Col10a1* genotype and genetic background			
	129/SvJ (*n*)		C57BL/6-129/SvJ (*n*)	
2 d	+/+ (7)	−/− (7)	+/+ (8)	−/− (8)
Femur shaft	110.54 ± 7.87	75.88 ± 7.42* ($P = 0.026$)	80.48 ± 3.6	51.73 ± 6.43* ($P = 0.022$)
4 wk	+/+ (5)	−/− (10)	+/+ (13)	−/− (13)
Femur head	141.66 ± 13.57	199.74 ± 5.83* ($P = 0.028$)	163.42 ± 4.97	161.76 ± 6.11
Shaft-head junction	116.72 ± 22.81	169.42 ± 8.11‡ ($P = 0.058$)	140.09 ± 6.57	152.42 ± 5.03
Femur shaft	12.07 ± 5.32	35.66 ± 8.12§ ($P = 0.054$)	12.57 ± 2.45	10.56 ± 2.04

The mineral content of the femur (expressed as the radiographic opacity) of mutant mice of 129/SvJ and C57BL/6-129/SvJ hybrid background were measured. Values represent mean ± SEM, unit in pixels; n = number of mice analyzed; *pp*, postpartum; +/+, wild-type; −/−, homozygous null mutant.
*Significant difference, $P < 0.05$ by K-S test;
‡ and §, P values marginally significant by K-S test.

regulate and influence the mineralization process and contribute to the unique architecture of bone is limited (Erlebacher et al., 1995). The molecular bases underlying the pathology of many forms of chondrodysplasia are also poorly understood (Horton and Hecht, 1993).

Despite the correlation between collagen X expression and endochondral ossification, a definition of its exact role has proved elusive. Also difficult to reconcile and explain has been the apparently contradictory consequences of mutations in the genes which result in collagen X deficiency, in human, and in mouse. Biochemical and cell transfection studies support the suggestion that in human SMCD, mutations in the NC1 domain cause depletion of collagen X because of a failure in assembly and secretion (Chan et al., 1995, 1996). Yet mice lacking collagen X have been reported to appear normal and do not develop SMCD (Rosati et al., 1994).

In this study we have shown that collagen X deficiency in mice does have phenotypic consequences which partly resemble SMCD, reducing the apparent discrepancy in phenotype between human and mouse. Intriguingly, the major impact of collagen X deficiency does not lie in its site of expression, the hypertrophic zone, but rather affects other zones of the growth plate and bone. We have found that the consequence of loss of collagen X in mutant mice is a major change in the distribution of matrix materials within the epiphyseal cartilage. Other features of collagen X deficiency are a significant reduction in the thickness of the resting zone and articular cartilage, an altered trabecular structure, and the bone content of femur bone. In particular, we find that collagen X deficient mice do develop *coxa vara*, one of phenotypic changes common in human SMCD. Notably, the genetic background of the mice is involved in the variability of some of the phenotypic consequences of the *Col10a1* mutation. An inbred background gave higher degree of penetrance and expressivity of the phenotype as shown in the trabecular morphological alteration, bone content measurement, and the occurence of *coxa vara* in the mutants. Variability of phenotypes has been reported previously in other "knock-out" studies (Liu et al., 1993; Ramírez-Solis et al., 1993), but it is still difficult to assess the cause for this.

A Hypothesis for the Function of Collagen X

Our data suggest that the underlying cause of these phenotypic changes could be related to the abnormal distribution of proteoglycans and matrix vesicles to nonhypertrophic regions of epiphyseal cartilage in the absence of collagen X. This altered distribution of matrix components may have arisen by diffusion from the hypertrophic zone or by displacement as the result of forces generated by rapid endochondral bone growth and initial perambulation. The changes in distribution of matrix components would alter the physical properties of the resting zone of growth plate cartilage and therefore its resilience to compression. In older animals articular cartilage thickness is reduced. Since collagen X is present in articular cartilage of wild-type mice at 4 wk and older (Cheah, K.S.E., unpublished data), these changes could be caused by the altered matrix composition in mutants. The persistent cartilaginous matrix in mutant trabeculae may reflect a different rate of replacement of an altered cartilage matrix by bone, in the absence of collagen X.

The alterations in bone content seen in mutants may be secondary effects due to the redistribution of matrix components in the absence of collagen X which results in a different pattern and regulation of the mineralization and remodeling process. The regulation of mineralization in cartilage and bone is complex and poorly understood, but collagens, proteoglycans, and matrix molecules are clearly involved in this process (Boskey, 1992). Matrix-mineral interactions within the hypertrophic zone of growth plate also regulate the size and type of hydroxyapatite crystal formation in bone during endochondral ossification (Boskey, 1992). Apart from their contribution to matrix structure in providing resilience under compressive force, proteoglycans are not initiators of mineralization but are proposed to play a role in mineralization by regulating hydroxyapatite growth and orientation (Boskey, 1992; Hunter, 1991).

Matrix vesicles are extracellular, cell-derived, membrane-bound microstructures containing mineral and alkaline phosphatase. These vesicles are abundant in the inter-territorial matrix in the upper hypertrophic zone and are proposed to be the initial nucleational foci for mineralization (Anderson, 1995). Matrix vesicles in the growth plate are associated with proteoglycans (Wu et al., 1991) and can bind to both collagens II and X (Kirsch and Wuthier, 1994; Kirsch et al., 1994). It has also been shown that the interaction between collagen II and X with matrix vesicles activates the influx of Ca^{++} into matrix vesicles suggesting a regulatory role of collagen X in mineralization (Kirsch and Wuthier, 1994; Kirsch et al., 1994).

Thus, the observed abnormal trabecular structure, retention of cartilaginous matrix within trabeculae and altered bone content in the mutant may reflect perturbation of both the normal patterns of matrix remodeling and mineral deposition caused by the altered distribution of matrix vesicles and proteoglycans within the growth plate in the absence of collagen X. Bone mineralization is thought to occur in two phases, initially via matrix vesicles for the formation of hydroxyapatite, and later through nucleation at collagen fibrils for the proliferation of mineral crystal within the extracelluar matrix (Anderson, 1995; Christofferson and Landis, 1991). The increased bone content observed at 4 wk may be a consequence of improperly regulated secondary mineralization caused by the altered matrix composition of the cartilaginous remnants in bone.

Taking all the data together, we hypothesize that collagen X is important for the compartmentalization of matrix components to the hypertrophic zone of growth cartilage, providing the proper environment for mineralization and bone remodeling. The hexagonal lattice structure proposed for collagen X (Kwan et al., 1991) and its affinity for proteoglycans (Chen et al., 1992) and collagen fibrils (Poole and Pidoux, 1989; Schmid and Linsenmayer, 1990) would be consistent with a role in compartmentalization. Collagen X may act as a pericellular network retaining or trapping the necessary types and amounts of matrix components, including the matrix vesicles and proteoglycans in the correct location of the hypertrophic zone of the growth plate, promoting initiation of normal mineralization. Thus, in the absence of collagen X, there is wider spread distribution of matrix components normally restricted to, or more concentrated in, the hypertrophic zone. As secondary consequences, this improper distribution of matrix molecules alters the structure of newly formed bone as well as the physical properties of cartilage, resulting in compression and deformation of parts of the growth plate. This hypothesis would reconcile the previously proposed differing views of the function of collagen X as a structural molecule providing support and as a regulator of mineralization.

Implications for the Molecular Mechanisms Underlying SMCD and Collagen X Mutations in Humans

With the increasing use of gene targeting in the mouse to produce models for understanding the molecular mechanisms underlying human disease, it has become increasingly important to assess how closely phenotypic consequences of mutations in mouse and man resemble each other. Our results show collagen X deficiency in mice does have phenotypic consequences which partly resemble SMCD, such as persistence of cartilage in trabecular bone and abnormalities in mineralization. The development of *coxa vara* is thought to be caused by a weakness of the growth plate in the metaphyses. The alterations in bone content and trabecular stucture in the mouse mutants may result in reduced strength of the bone against compressive force later in life and cause the onset of the *coxa vara.* The identification of *coxa vara* in the mutants, albeit at a later stage of onset than in human, suggests that collagen X deficiency does lead to weakening of the growth plate which would be consistent with a supportive role for the protein. In addition the data provides in vivo evidence supporting reduced collagen X levels as the cause of SMCD phenotype (Warman et al., 1993; Chan et al., 1995). In human metaphyseal chondrodysplasias, the extent of varus angulation is rarely equal on both sides. The varying incidence of *coxa vara* in the mouse mutants resembles the wide range of abnormality found in human SMCD which is, in any event, a relatively mild form of chondrodysplasia reviewed by Horton and Hecht (1993) and Lachman et al. (1988).

The reason for the late onset of *coxa vara* and the relatively milder phenotypic changes in collagen X mutant mice is not fully understood. The late onset of the defect in the mutant mice compared with the SMCD patients may be related to the differences in loading of the growth plate between man, a biped and mouse, a quadriped. However, the collagen X content in SMCD growth plates has not been determined. In addition it is not known if synthesizing abnormal α1(X) collagen chains which cannot assemble, has additional effects on hypertrophic chondrocytes, affecting their growth. It would therefore be important to compare the phenotypic consequences of the null with a SMCD mutation in mice.

An important issue raised is the relative mildness of phenotype in the null mutants compared with the SMD-like transgenic mice. Depletion of collagen X molecules caused by dominant interference with the normal assembly of the mouse protein by truncated chicken α1(X) chains has been proposed to cause the SMD-like phenotype in transgenic mice (Jacenko et al., 1993*b*), including compression of hypertrophic growth plate cartilage and a decrease in newly formed trabecular bone. An alternative explanation of the SMD-like phenotype is that the truncated chicken α1(X) collagen chains cause a dominant negative effect because of the deposition of abnormal collagen X in the matrix. The ability of α1(X) chains with internal deletions within the helix to assemble with normal chains as heterotrimers and be secreted, support the latter explanation (Chan et al., 1996). It is notable that the changes in trabecular structure observed in SMD-like transgenic mice (Jacenko et al., 1993*b*) were similar but more severe than in the collagen X null mutants. Our results suggest that different phenotypes of the null mutants and the SMD-like transgenic mice probably reflect differing severity of outcome of mutations resulting in loss vs gain of function.

Our data has yielded new insight into collagen X function. Questions remaining and currently being addressed, are the longer-term effects of the early matrix changes on susceptibility to osteoarthritis, bone remodeling, and frac-

ture repair since collagen X was shown to be upregulated in osteoarthritis (Von der Mark et al., 1992; Aigner et al., 1993; Hoyland et al., 1991) and transiently expressed in bone callus during fracture healing (Grant et al., 1987; Topping et al., 1994). Since all SMCD mutations found have been in the COOH-terminal noncollagenous domain reviewed in Chan et al. (1996), an additional question would be whether alterations elsewhere in the molecule may cause a different phenotype.

We also thank Robin Lovell-Badge, Peter Rowe, Alan Boyde, and Sheila Jones for advice and helpful discussion; Nevio Mok for expert assistance with electron microscopy and Man-Tong Lee and Ying-Yip Chui for invaluable help with histology.

This work was supported by the Arthritis & Rheumatism Council (UK) and the Wellcome Trust (UK). K.M. Kwan was a Croucher Foundation Scholar.

Received for publication 18 July 1996 and in revised form 15 October 1996.

References

Aigner, T., E. Reichenberger, W. Bertling, T. Kirsch, H. Stöss, and K. Von der Mark. 1993. Type X collagen expression in osteoarthritic and rheumatoid articular cartilage. *Virchows Arch. B Cell Pathol.* 63:205–211.

Anderson, H.C. 1989. Biology of disease. Mechanism of mineral formation in bone. *Lab. Invest.* 60:320–330.

Anderson, H.C. 1995. Molecular biology of matrix vesicles. *Clin. Orthop. Rel. Res.* 314:266–280.

Bonen, D.K., and T.M. Schmid. 1991. Elevated extracellular calcium concentrations induce type X collagen synthesis in chondrocyte cultures. *J. Cell Biol.* 115:1171–1178.

Boskey, A.L. 1992. Mineral-matrix interactions in bone and cartilage. *Clin. Orthop. Rel. Res.* 281:244–274.

Chan, D., W.G. Cole, J.G. Rogers, and J.F. Bateman. 1995. Type x collagen multimer assembly in vitro is prevented by a gly^{618} to val mutation in the α1(X) NC1 domain resulting in Schmid metaphyseal chondrodysplasia. *J. Biol. Chem.* 270:4558–4562.

Chan, D., Y.M. Weng, A.M. Hocking, S. Golub, D.J. McQuillan, and J.F. Bateman. 1996. Site-directed mutagenesis of human type X collagen: expression of α1(X) NC1, NC2, and helical mutations in vitro and in transfected cells. *J. Biol. Chem.* In press.

Cheah, K.S.E., E.T. Lau, P.K.C. Au, and P.P.L. Tam. 1991. Expression of the mouse α1(II) collagen gene is not restricted to cartilage during development. *Development.* 111:945–953.

Cheah, K.S.E., K.M. Kwan, M. Pang, S. Zhou, S.K. Cowan, R.Y.C. Kong, B.R. Olsen, and P.P.L. Tam. 1995. Altered matrix structure and bone density in collagen X null mice. *Ann. NY Acad. Sci.* In press.

Chen, Q., C. Linsenmayer, H. Gu, T.M. Schmid, and T.F. Linsenmayer. 1992. Domains of type X collagen: alteration of cartilage matrix by fibril association and proteoglycan accumulation. *J. Cell Biol.* 117:687–694.

Christofferson, J., and W.J. Landis. 1991. A contribution with review to the description of mineralization of bone and other calcified tissues in vivo. *Anat. Rec.* 230:435–450.

Erlebacher, A., E.H. Filvaroff, S.E. Gitelman, and R. Derynck. 1995. Toward a molecular understanding of skeletal development. *Cell.* 80:371–378.

Gibson, G.J., C.H. Bearman, and M.H. Flint. 1986. The immunoperoxidase localization of type X collagen in chick cartilage and lung. *Coll. Rel. Res.* 6: 163–184.

Grant, W.T., G.-J. Wang, and G. Balian. 1987. Type X collagen synthesis during endochondral ossification in fracture repair. *J. Biol. Chem.* 262:9844–9849.

Horton, W.A., and J.T. Hecht. 1993. The chondrodysplasias. *In* Connective Tissue and Its Heritable Disorders, Molecular Genetic and Medical Aspects. P.M. Royce and B. Steinmann, editors. Wiley-Liss, New York. 641–675.

Hoyland, J., J.T. Thomas, R. Donn, A. Marriott, S. Ayad, R. Boot-Handford, M.E. Grant, and A.J. Freemont. 1991. Distribution of type X collagen mRNA in normal and osteoarthritic human cartilage. *Bone Miner.* 15:151–164.

Hunter, G.K. 1991. Role of proteoglycan in the provisional calcification of cartilage. *Clin. Orthop. Rel. Res.* 262:256–280.

Hunziker, E.B., W. Herrmann, and R.K. Schenck. 1982. Improved cartilage fixation by ruthenium hexammine trichloride (RHT). A prerequisite for morphometry in growth cartilage. *J. Ultrastruct. Res.* 81:1–12.

Iannotti, J.P. 1990. Growth plate physiology and pathology. *Orthop. Clin. North Am.* 21:1–17.

Jacenko, O., P. LuValle, K. Solum, and B.R. Olsen. 1993*a.* A dominant negative mutation in the α1(X) collagen gene produces spondylometaphyseal defects in mice. *Prog. Clin. Biol. Res.* 383B:427–436.

Jacenko, O., P.A. LuValle, and B.R. Olsen. 1993*b.* Spondylometaphyseal dysplasia in mice carrying a dominant negative mutation in a matrix protein specific for cartilage-to-bone transition. *Nature (Lond.).* 365:56–61.

Kirsch, T., and M. Pfäffle. 1992. Selective binding of anchorin CII (annexin V) to type II and X collagen and to chondrocalcin (C-propeptide of type II collagen): implications for anchoring function between matrix vesicles and matrix proteins. *FEBS Lett.* 310:143–147.

Kirsch, T., and R.E. Wuthier. 1994. Stimulation of calcification of growth plate cartilage matrix vesicles by binding to type II and X collagens. *J. Biol. Chem.* 269:11462–11469.

Kirsch, T., B. Swoboda, and K. Von der Mark. 1992. Ascorbate independent differentiation of human chondrocytes in vitro: simultaneous expression of types I and X collagen and matrix mineralization. *Differentiation.* 52:89–100.

Kirsch, T., Y. Ishikawa, F. Mwale, and R.E. Wuthier. 1994. Roles of the nucleational core complex and collagens (types II and X) in calcification of growth plate cartilage matrix vesicles. *J. Biol. Chem.* 269:20103–20109.

Kong, R.Y.C., K.M. Kwan, E.T. Lau, J.T. Thomas, R.P. Boot-Handford, M.E. Grant, and K.S.E. Cheah. 1993. Intron-exon structure, alternative use of promoter and expression of the mouse collagen X gene, *Col10a-1. Eur. J. Biochem.* 213:99–111.

Kwan, A.P.L., C.E. Cummings, J.A. Chapman, and M.E. Grant. 1991. Macromolecular organization of chicken type X collagen in vitro. *J. Cell Biol.* 14: 597–604.

Lachman, R.S., D.L. Rimoin, and J. Spranger. 1988. Metaphyseal chondrodysplasia, Schmid type clinical and radiographic deliniation with a review of literature. *Pediatr. Radiol.* 18:93–102.

Liu, J.-P., J. Baker, A.S. Perkins, E.J. Robertson, and A. Efstratiadis. 1993. Mice carrying null mutations of the genes encoding insulin-like growth factor I (*Igf-1*) and type 1 IGF receptor (*Igf1r*). *Cell.* 75:59–72.

Lovell-Badge, R.H. 1987. Introduction of DNA into embryonic stem cells. *In* Teratocarcinomas and Embryonic Stem Cells - a Practical Approach. E.J. Robertson, editor. IRL press, Oxford. 153–182.

Mayne, R., and M.H. Irwin. 1986. Collagen types in cartilage. *In* Articular Cartilage Biochemistry. K.E. Kuettner, R. Schleyerbach, and V.C. Hascall, editors. Raven Press, New York. 23–35.

McIntosh, I., M.H. Abbott, and C.A. Francomano. 1995. Concentration of mutations causing Schmid metaphyseal chondrodysplasia in the C-terminal noncollagenous domain of type X collagen. *Hum. Mutat.* 5:121–125.

Muragaki, Y., M.G. Mattei, N. Yamaguchi, B.R. Olsen, and Y. Ninomiya. 1991*a.* The complete primary structure of the human alpha 1(VIII) chain and assignment of its gene (COL8A1) to chromosome 3. *Eur. J. Biochem.* 197:615–622.

Muragaki, Y., O. Jacenko, S.S. Apte, M.G. Mattei, Y. Ninomiya, and B.R. Olsen. 1991*b.* The alpha 2(VIII) collagen gene. A novel member of the short chain collagen family located on the human chromosome 1. *J. Biol. Chem.* 266:7721–7727.

Poole, A.R., and I. Pidoux. 1989. Immunoelectron microscopic studies of type X collagen in endochondral ossification. *J. Cell Biol.* 109:2547–2554.

Ramírez-Solis, R., H. Zheng, J. Whiting, R. Krumlauf, and A. Bradley. 1993. *Hoxb-4 (Hox-2.6)* mutant mice show homeotic transformation of a cervical vertebra and defects in the closure of the sternal rudiments. *Cell.* 73:279–294.

Rosati, R., G.S.B. Horan, G.J. Pinero, S. Garofalo, D.R. Keene, W.A. Horton, B. De Crombrugghe, and R.R. Behringer. 1994. Normal long bone growth and development in type x collagen-null mice. *Nature Genet.* 8:129–135.

Schmid, T.M., and T.F. Linsenmayer. 1985. Immunohistochemical localization of short chain cartilage collagen (type X) in avian tissues. *J. Cell Biol.* 100: 598–605.

Schmid, T.M., and T.F. Linsenmayer. 1987. Type X collagen. *In* Structure and Function of Collagen Types. R. Mayne, and R.E. Burgeson, editors. Academic Press, Orlando, FL. 223–259.

Schmid, T.M., and T.F. Linsenmayer. 1990. Immunoelectron microscopy of type X collagen: supramolecular forms within embryonic chick cartilage. *Dev. Biol.* 138:53–62.

Schmid, T.M., R.G. Popp, and T.F. Linsenmayer. 1990. Hypertrophic cartilage matrix: Type X collagen, supramolecular assembly, and calcification. *Ann. NY Acad. Sci.* 580:64–73.

Schmid, T.M., D.K. Bonen, L. Luchene, and T.F. Linsenmayer. 1991. Late events in chondrocyte differentiation: hypertrophy, type X collagen synthesis and matrix calcification. *In Vivo.* 5:533–540.

Topping, R.E., M.E. Bolander, and G. Balian. 1994. Type X collagen in fracture callus and the effects of experimental diabetes. *Clin. Orthop.* 308:220–228.

Von der Mark, K., T. Kirsch, A. Nerlich, A. Kuss, G. Weseloh, K. Glückert, and H. Stöss. 1992. Type X collagen synthesis in human osteoarthritic cartilage: indication of chondrocyte hypertrophy. *Arthritis Rheum.* 35:806–811.

Wallis, G.A. 1993. Here today, bone tomorrow. *Curr. Biol.* 3:687–689.

Wallis, G.A., B. Rash, W.A. Sweetman, J.T. Thomas, M. Super, G. Evans, M.E. Grant, and R.P. Boot-Handford. 1994. Amino acid substitutions of conserved residues in the carboxyl-terminal domain of the α1(X) chain of type X collagen occur in two unrelated families with metaphyseal chondrodysplasia type Schmid. *Am. J. Hum. Genet.* 54:169–178.

Warman, M.L., M. Abbott, S.S. Apte, T. Hefferon, I. McIntosh, D.H. Cohn, J.T. Hecht, B.R. Olsen, and C.A. Francomano. 1993. A type X collagen mutation causes Schmid metaphyseal chondrodysplasia. *Nature Genet.* 5:79–82.

Wu, L.N.Y., B.R. Genge, and R.E. Wuthier. 1991. Association between proteoglycans and matrix vesicles in the extracellular matrix of growth plate cartilage. *J. Biol. Chem.* 266:1187–1194.